NANO LETTERS

Letter

pubs.acs.org/NanoLett

Free-Standing Single-Molecule Thick Crystals Consisting of Linear Long-Chain Polymers

Renwei Liu,[†,‡] Suna Fan,[†,‡] Dongdong Xiao,[‡] Jin Zhang,[‡] Mengzhou Liao,[‡] Shansheng Yu,[†] Fanling Meng,[†] Baoli Liu,[‡] Lin Gu,[‡] Sheng Meng,[‡] Guangyu Zhang,[‡] Weitao Zheng,[†] Shuxin Hu,*[,‡] and Ming Li*[,‡,§]

[†]Key Laboratory of Automobile Materials of MOE, State Key Laboratory of Automotive Simulation and Control, and Department of Materials Science, Jilin University, Changchun, Jilin 130000, China

[‡]Beijing National Laboratory for Condensed Matter Physics, Institute of Physics, Chinese Academy of Sciences, Beijing 100190, China

[§]School of Physical Sciences, University of Chinese Academy of Sciences, Beijing 100190, China

S *Supporting Information*

ABSTRACT: Organic two-dimensional (2D) crystals are fundamentally important for development of future devices. Despite that more than a half of man-made products contain polymers, 2D crystals consisting of long linear chains have yet to be explored. Here we report on the fabrication of 2D polyaniline (PANI) crystals via rational electrochemical polymerization followed by liquid-phase exfoliation. The 2D PANI is molecularly thin (~0.8 nm) and composed of PANI chains with a number-average molecular weight of ~31 000. The chains are parallel to each other with the benzene rings standing almost vertically to the surface, implying a face-to-face arrangement of the neighboring chains held together by abundant $\pi-\pi$ interactions augmented with hydrogen bonds. The 2D PANI can be readily transferred to various solid surfaces and exhibit interesting electrical and optical properties, suggesting that they would be potentially useful in photoelectronic devices and other applications.

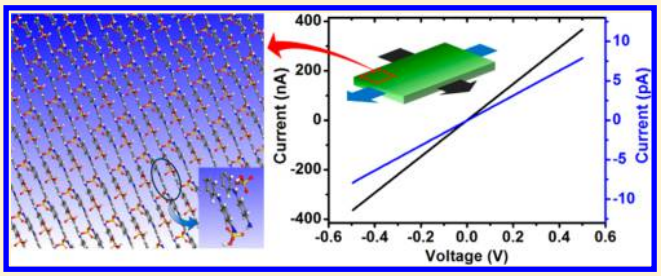

KEYWORDS: *Two-dimensional crystals, anisotropic electrical conductivity, electrochemical polymerization, liquid-phase exfoliation, polyaniline*

The discovery of graphene triggered enormous enthusiasms for 2D materials with most interest being focused on inorganic materials such as monolayered black phosphorus, hexagonal boron nitride, transition metal dichalcogenides, and so on.[1−4] Inspired by the structure of 2D inorganic materials, chemists have made intense efforts to synthesize properly functionalized organic monomers that react in two orthogonal directions to construct 2D networks.[5−8] The products usually have limited size because networks formed locally might sterically hinder each other during further growth.[9,10] Besides various functionalized organic monomers, hundreds of thousands of simple organic monomers could be polymerized into linear chains. The family of 2D materials will be hence greatly expanded if they can be made of linear chains.[11] In addition, the difference in intra- and interchain interactions in such 2D materials will lead to anisotropic physical properties, facilitating new designs of molecular devices. To date, to the best of our knowledge subnanometer thick 2D crystals consisting of linear long-chain polymers have not yet been reported.

In the present work, we report on fabrication and structural analysis of the first 2D crystals composed of linear long-chains and study their optical and electrical properties. Two main approaches have been used to fabricate 2D materials. One is to directly synthesize the materials from monomers confined on surfaces or interfaces.[12,13] The approach provides outstanding analytical capability but produces only small sheets, usually with sizes less than a few hundred nanometers. Another approach is to exfoliate lamellar crystals.[5,6,14,15] Many linear polymers can crystallize into layered structures in which the chains are usually folded back and forth perpendicular to the layers.[16−18] This may render the exfoliation impossible (because the chains may run across many platelets) or would result in small platelets thicker than 10 nm. We hypothesized that one can make single-molecule thick materials by exfoliating a lamellar crystal consisting of extended chains that run parallel to the surface. In the search for potential candidates, we found that a few types of polyaniline (PANI) crystals have the demanded structure.[19−21] Moreover, as a conjugated polymer composed of benzene ring and amino group, PANI chains can support

Received: November 23, 2016
Revised: February 10, 2017
Published: February 15, 2017

DOI: 10.1021/acs.nanolett.6b04896
Nano Lett. 2017, 17, 1655−1659

interchain $\pi-\pi$ interactions and hydrogen bonds, favoring ordered structures.[22] In addition, bulk PANI is one of the most important conducting polymers that has attracted much attention for applications in various electronic devices because of their high conductivity, good environmental stability, and unusual doping/dedoping chemistry.[23,24]

We first adopted electrochemical polymerization method,[25] by which extended chain conformation can be obtained,[26] to produce lamellar PANI crystals (Figure S1). In practice, oriented growth is preferred in order to get large-area nanosheets via exfoliation. Our previous studies showed that highly oriented lamellar structures can be electrodeposited on polished silicon wafers (highly doped; resistivity ≈ 10 Ω·cm).[27,28] We used a similar strategy to deposit oriented lamellar PANI crystals. After deaeration of electrolyte by a dry nitrogen stream, the potential was shifted to 0.79 V versus the saturated calomel electrode (SCE). Higher potentials increased the probability of side reactions and caused the polymer to degrade,[29] resulting in disordered structures. Although PANI could be deposited at a potential lower than 0.7 V, an even lower potential might lead to a polymerization rate that is too low to compete the side reactions, leading to poor films that could not even be exfoliated. We found that when the potential was set to 0.7−0.8 V the polymerization went directly toward linear PANI, favoring formation of layered PANI crystals. Because high monomer concentration may increase the probability of chain transfer between the monomers and the growing polymeric species to shorten the chain length,[30,31] we set the aniline concentration to as low as 0.1 M in order to obtain chains with high molecular weight. The relative number-average molecular weight and polydispersity index (PDI) of PANI polymerized at 0.79 V were measured to be about 31000 and 1.98 by gel permeation chromatography (GPC) (Figure S2a and Table S1), respectively. Although the counterion type of the dopant does not govern the electron transfer rate of PANI, it has a direct impact on the structure of the chain and hence the morphology of the crystal. Sulfuric acid has a tetrahedral structure, favoring the formation of O···H—N type hydrogen bonds to bridge the amino groups in adjacent chains, promoting an ordered interchain arrangement.[32] In addition, a low pH (~0.3) of the electrolyte supplied by 0.5 M H_2SO_4 avoided the formation of phenazine-like units, which is the main cross-linking mode of PANI.[33,34] All together, the optimized growth parameters, namely, low monomer concentration, low pH value, proper dopant, and adequately applied potential, resulted in the linear PANI and a 2D growth mode on the electrode, as can be seen from the AFM images of a PANI crystal taken at the initial nucleation stage (Figure 1a,b) and the later layered growth stage (Figure 1c). Terraces are clearly visible in the AFM images, the thinnest of which is only about 7.9 Å (Figure S3). The scanning electron microscopy (SEM) of the as-grown crystals indicates that they are indeed composed of well-aligned platelets (Figure S1c).

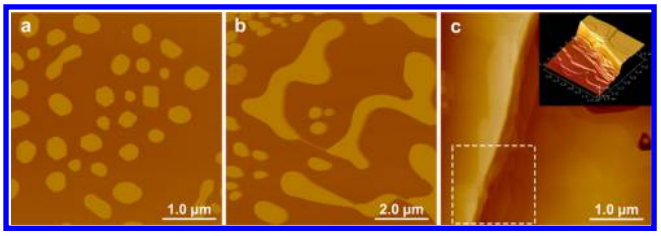

Figure 1. AFM images of the growth frontiers after different electrochemical deposition time: (a) 50, (b) 200, and (c) 1000 s. Inset: 3D image of the white square in (c).

We used liquid-phase exfoliation to break down the PANI crystals. To this end, we tested a few solvents that we selected according to the Hansen solubility parameter theory[35] and found that isopropanol works well to exfoliate the PANI crystals. We subjected the crystals to isopropanol and shook the crystals for a few days at room temperature (Figure 2a) in order to achieve full exfoliation down to individual monolayers[14] (Figure S4). The swelled crystals in isopropanol were then sonicated for 10 min. After centrifugation, the supernatants contained PANI sheets were stable for a few weeks. The thickness of the PANI sheets depend on the power and duration of the sonication (Figure 2b,c and Figures S6−S9). Because ultrathin organic films are usually sensitive to electron beams,[14] we prepared few-layer PANI sheets and transferred them to lacey-carbon-coated grids for TEM observations. Some nanosheets were sufficiently thin and hence exhibited wrinkles and folded regions (Figure 2c), which is a common feature of large-size 2D materials.[11,36] We also transferred the PANI sheets onto fresh mica, SiO_2 (300 nm)/silicon, highly oriented pyrolytic graphite (HOPG) and SiC surfaces (Figures S6−S9) to produce solid-supported 2D PANI. The thinnest sheets we measured are only 8.5 Å thick (Figure 2d), which is equal to the minimal thickness of the terraces in Figure S3, indicating that single-molecule-thick PANI sheets with micron size are obtained. It is worth noting that a narrow molecular weight distribtion, rather than the molecule weight itself, is of importance for growing high-quality crystals and hence high-quanlity 2D PANI (Figure S2 and S5, Table S1).

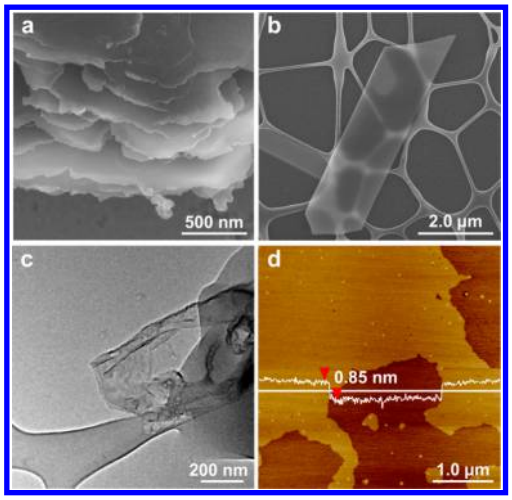

Figure 2. Exfoliation and transfer of 2D PANI crystals. (a) SEM image of a PANI crystal swelled in isopropanol. (b,c) SEM and TEM images of thick and thin PANI sheets, respectively. (d) AFM image of a monolayer PANI on mica and the height profile along the line indicated in the image.

The regular lattice fringes in the high-resolution TEM (HRTEM) images indicated that the 2D PANI layers consist of linear long-chains (Figure 3a) rather than short oligomers, making our products differ from other two-dimensionally self-assembled materials[37,38] or organic frameworks.[39−41] The chains all lie parallel to the surface, contrary to those in most polymer lamellar crystals that fold back and forth perpendicular to the surface.[16−18] The interchain spacing is ~3.2 Å, implying

DOI: 10.1021/acs.nanolett.6b04896
Nano Lett. 2017, 17, 1655−1659

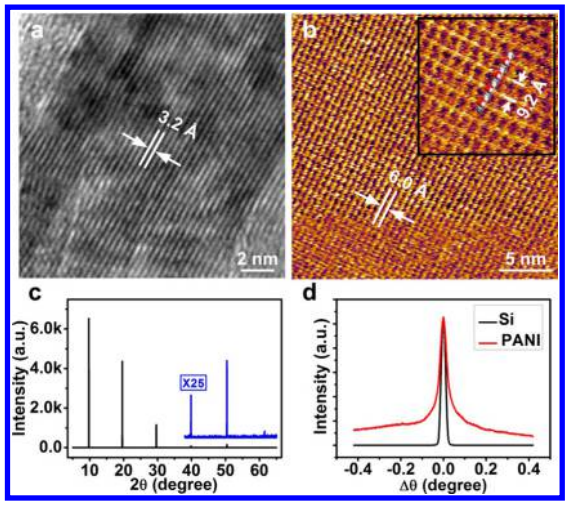

Figure 3. (a) High-resolution TEM image and (b) AFM image of the PANI sheets. Inset is the zoom-in AFM image of (b). (c) X-ray reflection (XRR) pattern of an as-grown crystal. (d) Rocking curve around the first Bragg peak whose width is limited by the instrumental resolution.

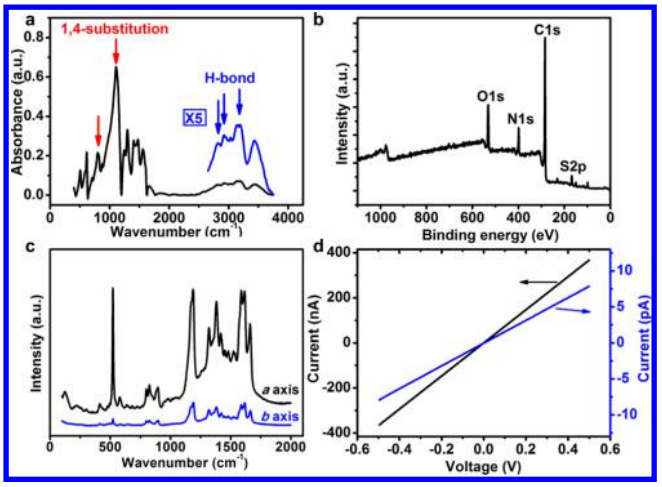

Figure 4. (a) FTIR, (b) XPS spectrum, and (c) polarized Raman scattering spectra of the PANI crystal. (d) $I-V$ curves measured in directions along (black line, a axis of the lattice) and perpendicular to the PANI chains (blue line, b axis of the lattice).

a face-to-face arrangement of the neighboring chains.[19,42] The structure is confirmed by the high-resolution AFM (HRAFM) observations (Figure 3b) in which the observed interline distance is two folds of that in the HRTEM. The interactions between the aromatic rings result in an offset face-to-face geometry of the chains.[43,44] A chain at the lower level sandwiched by two chains at the upper level is invisible in the HRAFM images. The zoom-in AFM image (inset of Figure 3b) exhibits a rectangular lattice with 2D lattice constants of a = 9.2 ± 0.1 Å and b = 6.0 ± 0.1 Å. Here, the lattice axes a and b are along and perpendicular to the molecular chains, respectively. The X-ray reflectivity (XRR) peaks of the as-grown crystals (Figure 3c) can be indexed as (00n), n = 1,2,3,... This, together with the rocking curve around the first Bragg peak (Figure 3d), reveals that the crystals are composed of highly ordered stacking of PANI monolayers which are all parallel to the surfaces of the substrates. The intermonolayer distance measured by XRR is 9.08 Å, indicating again that the thinnest sheets we obtained (Figure 2d) are single-molecule thick.

We applied Fourier transform infrared spectroscopy (FTIR) to characterize the molecular configuration in the crystals (Figure 4a). Peaks at 1107 and 810 cm^{-1} in the FTIR spectrum can be attributed to the in-plane and out-of-plane bending of C—H of the 1,4-substituted rings, respectively.[45,46] The absence of peaks (1115, 1060, 960, 895 cm^{-1}) for the C—H bending of the 1,2,4-trisubstituted rings affirms that the PANI chains consist solely of 1,4-substituted benzene rings.[47,48] That is, the PANI are linear polymer, ruling out a configuration of 2D covalent network in the 2D PANI. In addition, the quantitative analyses of the X-ray photoelectron spectroscopy (XPS) data (Figure 4b and Figure S10) reveal that the PANI sheets are composed of C, N, O and S elements only, with a S/N ratio very close to 1:2, indicating a high doping level.[25,49] Both the polarized Raman scattering (Figure 4c) and the electric conductivity (Figure 4d) reveal that the PANI exhibits anisotropic physical properties. The orientation of PANI chains in the crystals can be reflected by a depolarization ratio of Raman bands (ρ_{iso}), which is expressed as $I_{perpendicular}/I_{parallel}$. $I_{pendicular}$ is much stronger than $I_{parallel}$ with $\rho_{iso} \approx 5.6$. The electrical conductivity of few-layer PANI sheets was measured with a two-electrode method (Figure 4d and Figure S13). It turned out that the PANI has a much higher conductivity along the chains (0.32 S·cm^{-1}) than perpendicular to the chains (3.58 × 10^{-5} S·cm^{-1}).

In order to uncover which types of interactions are involved to hold the linear PANI chains together to form the 2D crystal, we performed first-principles density functional theory calculations of monolayer, bilayer and bulk PANI (see Supporting Information for details). After full relaxation of lattice constants and atomic positions, the optimized geometry yielded a simple triclinic lattice with parameters a = 10.5 Å, b = 6.5 Å, c = 11.0 Å, α = 92°, β = 94°, and γ = 90°, which are in excellent agreement with the experimental data above. The atomic structure of a monolayer PANI is depicted in Figure 5. The chains are parallel to each other with the benzene rings standing almost vertically to the 2D PANI. The adjacent chains are offset by 2.75 Å in the direction normal to the monolayer, explaining why HRAFM sees a 6 Å interchain spacing while the HRTEM sees a 3 Å interchain spacing (Figure 3a,b). It is consistent with the HRAFM result that the exposed bisulfate anions are at the corners of the rectangles, as indicated by the molecular model inserted in the image (Figure 3b). The calculations also indicated that the neighboring chains are bridged by bisulfate anions, which are very close to the amine groups to form O···H—N hydrogen bonds (Figure 5b,d). The existence of the hydrogen bonds was also confirmed by the FTIR data that exhibits a series of peaks at 2840, 2926, and 3190 cm^{-1} (Figure 4a). In addition, the calculated frontier orbitals (HOMO+LUMO) at the Γ point in the Brillouin zone suggest the existence of $\pi-\pi$ interactions between adjacent chains (Figure 5e). Taken together, it is the abundant $\pi-\pi$ interactions and the hydrogen bonds that hold the PANI chains together. Ultimately, the formation energy of bilayered PANI is calculated to be ~1.80 eV/nm^2, lower than that of bilayered graphene (~3.35 eV/nm^2). This is consistent with the fact that the electron-density map of a PANI bilayer shows no overlapping of the two constituent monolayers (Figure 5f).

We compared the optical properties of PANI sheets of different thicknesses. Figure 6a shows the differential reflectance ($\Delta R/R$) spectra, which are proportional to the

DOI: 10.1021/acs.nanolett.6b04896
Nano Lett. 2017, 17, 1655−1659

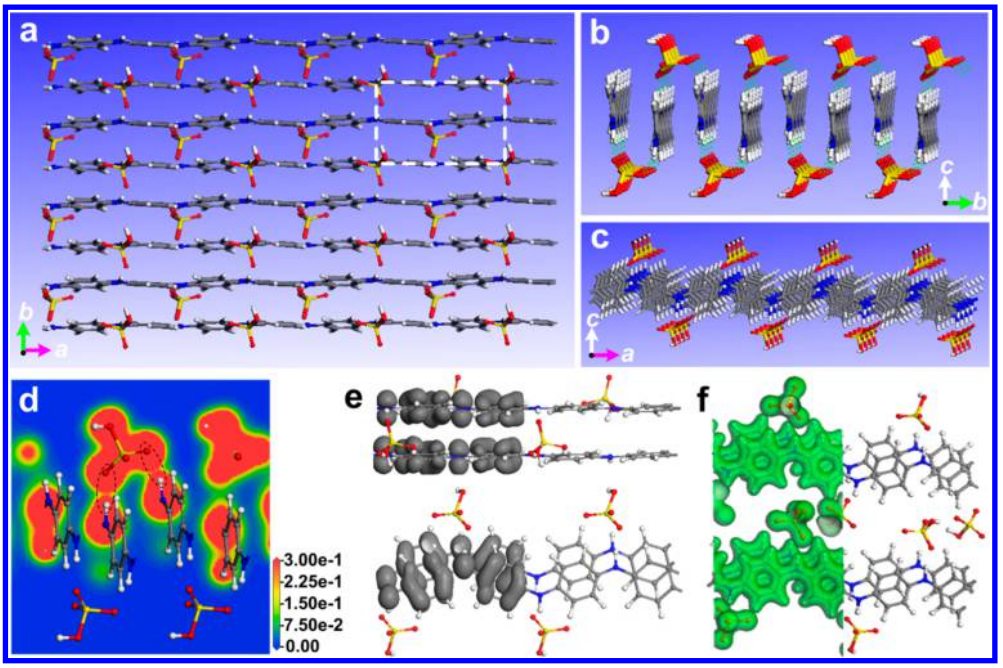

Figure 5. Atomic structures and interactions in PANI. (a–c) Top, side, and front views of a monolayer PANI. Gray, carbon; blue, nitrogen; yellow, sulfur; red, oxygen; white, hydrogen. Bisulfate ions link adjacent chains via hydrogen bonds (green dashed lines in b). (d) Electron density slice on a plane perpendicular to the chains indicates the hydrogen bonds. (e) Frontier orbitals at the Γ point in the Brillouin zone indicate π–π interactions. (f) Electron-density map of a bilayered PANI without overlapping of its constituent monolayers.

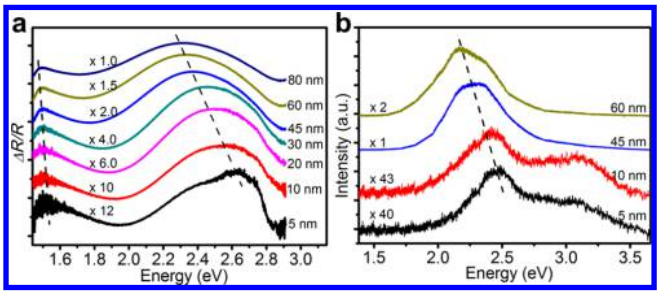

Figure 6. (a) Differential reflectance and (b) photoluminescence (PL) spectra (measured with an excitation wavelength of 325 nm) of the PANI sheets with different thicknesses. The spectra are enlarged by certain factors and shifted vertically to facilitate the comparison.

absorption of the sheets and could be regarded as absorption spectra.[50,51] Two absorption peaks centered at 1.53 and 2.63 eV were observed. The former was also observed in other reported bulk PANI and is believed to originate from the π-polaron transition.[52] The latter is somewhat complex and may be attributed partly to band nesting.[53] Further studies are required to understand the origin of this strong absorption at higher energies. All the absorption peaks display a clear blueshift with the decreasing thickness, which is similar to that observed for other 2D materials.[50,54] We also investigated the photoluminescence (PL) properties of the PANI sheets (Figure 6b). The thicker sheet (~60 nm) exhibits a broad emission peak at 2.18 eV. This peak shifts toward higher energy with decreasing sheet thickness. What is worth noting is that PANI sheets exhibit a new emission peak at about 3.09 eV when they are sufficiently thin. This thickness-dependent difference of the PL spectra for PANI sheets might motivate to open up new applications in photonics devices.

In summary, 2D PANI crystals consisting of linear long-chains can be stabilized via noncovalent bonds. The polymer chains lie parallel to the 2D crystal with the benzene rings in the chains standing face-to-face between neighboring chains, favoring π–π interactions. The neighboring chains are further bridged by bisulfate ions through hydrogen bonds. The 2D PANI crystals are stable in proper solvents and can be readily transferred to various solid surfaces. The conductivity of 2D PANI along the chains is much higher than that perpendicular to the chains. All the absorption and emission peaks display clear blueshift with decreasing thickness. In addition, a new emission peak is observed when the sheet is sufficiently thin. One expects that the use of such 2D PANI as active components in devices would improve the functionalities of conventional polymers.

■ ASSOCIATED CONTENT

Supporting Information

The Supporting Information is available free of charge on the ACS Publications website at DOI: 10.1021/acs.nanolett.6b04896.

Additional experimental details, first-principles density functional theory calculations, and additional experimental results (PDF)

■ AUTHOR INFORMATION

Corresponding Authors

*E-mail: mingli@iphy.ac.cn.
*E-mail: hushuxin@iphy.ac.cn.

ORCID

Ming Li: 0000-0002-5328-5826

Author Contributions

The manuscript was written through contributions of all authors. All authors have given approval to the final version of the manuscript. R.L. and S.F. contributed equally.

DOI: 10.1021/acs.nanolett.6b04896
Nano Lett. 2017, 17, 1655–1659

Notes

The authors declare no competing financial interest.

■ ACKNOWLEDGMENTS

This work was supported by the National Science Foundation of China (Grants 11574382, 51372095, and 91323304) and by the Key Research Program of Frontier Sciences, CAS (Grant QYZDJ-SSW-SYS014). J.Z. and S.M. acknowledge supports from MOST (Grant 2012CB921403). We thank Professors Z. X. Cao and L. Lv for stimulating discussions. We also thank Professor G. Wang for the SiC wafers and Professor K. H. Wu for the HOPG wafers.

■ REFERENCES

(1) Nag, A.; Raidongia, K.; Hermbram, K. P. S. S.; Datta, R.; Waghmare, U. V.; Rao, C. N. R. *ACS Nano* **2010**, *4*, 1539−1544.
(2) Rao, C. N.; Matte, H. S.; Maitra, U. *Angew. Chem., Int. Ed.* **2013**, *52*, 13162−13185.
(3) Zhang, A. Q.; Lieber, C. M. *Chem. Rev.* **2016**, *116*, 215−257.
(4) Cao, Y.; Liu, S.; Shen, Q.; Yan, K.; Li, P. J.; Xu, J. B.; Yu, D. P.; Steigerwald, M. L.; Nuckolls, C.; Liu, Z. F.; Guo, X. F. *Adv. Funct. Mater.* **2009**, *19*, 2743−2748.
(5) Kory, M. J.; Worle, M.; Weber, T.; Payamyar, P.; van de Poll, S. W.; Dshemuchadse, J.; Trapp, N.; Schluter, A. D. *Nat. Chem.* **2014**, *6*, 779−784.
(6) Kissel, P.; Murray, D. J.; Wulftange, W. J.; Catalano, V. J.; King, B. T. *Nat. Chem.* **2014**, *6*, 774−778.
(7) Dou, L.; Wong, A. B.; Yu, Y.; Lai, M.; Kornienko, N.; W, E. S.; Fu, A.; Bischak, C. G.; Ma, J.; Ding, T.; Ginsberg, N. S.; Wang, L. W.; Alivisatos, A. P.; Yang, P. D. *Science* **2015**, *349*, 1518−1521.
(8) Lee, C. H.; Schiros, T.; Santos, E. J.; Kim, B.; Yager, K. G.; Kang, S. J.; Lee, S.; Yu, J.; Watanabe, K.; Taniguchi, T.; Hone, J.; Kaxiras, E.; Nuckolls, C.; Kim, P. *Adv. Mater.* **2014**, *26*, 2812−2817.
(9) Perepichka, D. F.; Rosei, F. *Science* **2009**, *323*, 216−217.
(10) Guan, C. Z.; Wang, D.; Wan, L. J. *Chem. Commun.* **2012**, *48*, 2943−2945.
(11) Sakamoto, J.; Heijst, J. v.; Lukin, O.; Schluter, A. D. *Angew. Chem., Int. Ed.* **2009**, *48*, 1030−1069.
(12) Kley, C. S.; Cechal, J.; Kumagai, T.; Schramm, F.; Ruben, M.; Stepanow, S.; Kern, K. *J. Am. Chem. Soc.* **2012**, *134*, 6072−6075.
(13) Liu, X.; Guan, C.; Ding, S.; Wang, W.; Yan, H.; Wang, D.; Wan, L. *J. Am. Chem. Soc.* **2013**, *135*, 10470−10474.
(14) Kissel, P.; Erni, R.; Schweizer, W. B.; Rossell, M. D.; King, B. T.; Bauer, T.; Gotzinger, S.; Schluter, A. D.; Sakamoto, J. *Nat. Chem.* **2012**, *4*, 287−291.
(15) Chandra, S.; Kandambeth, S.; Biswal, B. P.; Lukose, B.; Kunjir, S. M.; Chaudhary, M.; Babarao, R.; Heine, T.; Banerjee, R. *J. Am. Chem. Soc.* **2013**, *135*, 17853−17861.
(16) Nakamura, J.; Kawaguchi, A. *Macromolecules* **2004**, *37*, 3725−3734.
(17) Zhu, L.; Cheng, S. Z. D.; Calhoun, B. H.; Ge, Q.; Quirk, R. P.; Thomas, E. L.; Hsiao, B. S.; Yeh, F.; Lotz, B. *J. Am. Chem. Soc.* **2000**, *122*, 5957−5967.
(18) Zhai, X.; Wang, W.; Ma, Z.; Wen, X.; Yuan, F.; Tang, X.; He, B. *Macromolecules* **2005**, *38*, 1717−1722.
(19) Wu, C.; Chiang, C. *CrystEngComm* **2011**, *13*, 1406−1409.
(20) Yan, Y.; Fang, J.; Zhang, Y.; Fan, H.; Wei, Z. *Macromol. Rapid Commun.* **2011**, *32*, 1640−1644.
(21) Choi, I. Y.; Lee, J.; Ahn, H.; Lee, J.; Choi, H. C.; Park, M. J. *Angew. Chem., Int. Ed.* **2015**, *54*, 10497−10501.
(22) Elemans, J. A.; Lei, S.; Feyter, S. D. *Angew. Chem., Int. Ed.* **2009**, *48*, 7298−7332.
(23) Zhang, H.; Wang, X.; Li, J.; Mo, Z.; Wang, F. *Polymer* **2009**, *50*, 2674−2679.
(24) Liang, L.; Liu, J.; Windisch, C. F., Jr.; Exarhos, G. J.; Lin, Y. *Angew. Chem., Int. Ed.* **2002**, *41*, 3665−3668.
(25) Feng, X.; Li, R.; Ma, Y.; Chen, R.; Shi, N.; Fan, Q.; Huang, W. *Adv. Funct. Mater.* **2011**, *21*, 2989−2996.
(26) Collard, D. M.; Stoakes, M. S. *Chem. Mater.* **1994**, *6*, 850−857.
(27) Xing, L. L.; Yuan, B.; Hu, S. X.; Zhang, Y. D.; Lu, Y.; Mai, Z. H.; Li, M. *J. Phys. Chem. C* **2008**, *112*, 3800−3804.
(28) Jing, H.; Li, X.; Lu, Y.; Mai, Z.; Li, M. *J. Phys. Chem. B* **2005**, *109*, 2881−2884.
(29) Lapkowski, M. *Synth. Met.* **1990**, *35*, 169−182.
(30) Mu, S.; Chen, C.; Wang, J. *Synth. Met.* **1997**, *88*, 249−254.
(31) Shi, G.; Jin, S.; Xue, G.; Li, C. *Science* **1995**, *267*, 994−996.
(32) Šeděnková, I.; Trchová, M.; Blinova, N. V.; Stejskal, J. *Thin Solid Films* **2006**, *515*, 1640−1646.
(33) Zujovic, Z. D.; Zhang, L.; Bowmaker, G. A.; Kilmartin, P. A.; Sejdic, J. T. *Macromolecules* **2008**, *41*, 3125−3135.
(34) Trchova, M.; Sedenkova, I.; Konyushenko, E. N.; Stejskal, J.; Holler, P.; Marjanovic, G. C. *J. Phys. Chem. B* **2006**, *110*, 9461−9468.
(35) Bergin, S. D.; Sun, Z.; Rickard, D.; Streich, P. V.; Hamilton, J. P.; Coleman, J. N. *ACS Nano* **2009**, *3*, 2340−2350.
(36) Meyer, J. C.; Geim, A. K.; Katsnelson, M. I.; Novoselov, K. S.; Booth, T. J.; Roth, S. *Nature* **2007**, *446*, 60−63.
(37) Nam, K. T.; Shelby, S. A.; Choi, P. H.; Marciel, A. B.; Chen, R.; Tan, L.; Chu, T. K.; Mesch, R. A.; Lee, B. C.; Connolly, M. D.; Kisielowski, C.; Zuckermann, R. N. *Nat. Mater.* **2010**, *9*, 454−460.
(38) Vybornyi, M.; Rudnev, A.; Häner, R. *Chem. Mater.* **2015**, *27*, 1426−1431.
(39) Zhuang, X.; Mai, Y.; Wu, D.; Zhang, F.; Feng, X. *Adv. Mater.* **2015**, *27*, 403−427.
(40) Xiang, Z.; Cao, D.; Dai, L. *Polym. Chem.* **2015**, *6*, 1896−1911.
(41) Mahmood, J.; Lee, E. K.; Jung, M.; Shin, D.; Choi, H. J.; Seo, J. M.; Jung, S. M.; Kim, D.; Li, F.; Lah, M. S.; Park, N.; Shin, H. J.; Oh, J. H.; Baek, J. B. *Proc. Natl. Acad. Sci. U. S. A.* **2016**, *113*, 7414−7419.
(42) Lee, Y.; Chang, C.; Yau, S.; Fan, L.; Yang, Y.; Yang, L. O.; Itaya, K. *J. Am. Chem. Soc.* **2009**, *131*, 6468−6474.
(43) Cubberley, M. S.; Iverson, B. L. *J. Am. Chem. Soc.* **2001**, *123*, 7560−7563.
(44) Curtis, M. D.; Cao, J.; Kampf, J. W. *J. Am. Chem. Soc.* **2004**, *126*, 4318−4328.
(45) Furukawa, Y.; Ueda, F.; Hyodo, Y.; Harada, I. *Macromolecules* **1988**, *21*, 1297−1305.
(46) Li, Y.; Zhao, X.; Xu, Q.; Zhang, Q.; Chen, D. *Langmuir* **2011**, *27*, 6458−6463.
(47) Tang, J.; Jing, X.; Wang, B.; Wang, F. *Synth. Met.* **1988**, *24*, 231−238.
(48) Stejskal, J.; Sapurina, I.; Trchová, M.; Konyushenko, E. N.; Holler, P. *Polymer* **2006**, *47*, 8253−8262.
(49) Han, M. G.; Cho, S. K.; Oh, S. G.; Im, S. S. *Synth. Met.* **2002**, *126*, 53−60.
(50) Dhakal, K. P.; Duong, D. L.; Lee, J.; Nam, H.; Kim, M.; Kan, M.; Lee, Y. H.; Kim, J. *Nanoscale* **2014**, *6*, 13028−13035.
(51) Mcintyre, J. D. E.; Aspnes, D. E. *Surf. Sci.* **1971**, *24*, 417−434.
(52) Jimenez, P.; Castell, P.; Sainz, R.; Anson, A.; Martinez, M. T.; Benito, A. M.; Maser, W. K. *J. Phys. Chem. B* **2010**, *114*, 1579−1585.
(53) Carvalho, A.; Ribeiro, R. M.; Castro Neto, A. H. *Phys. Rev. B: Condens. Matter Mater. Phys.* **2013**, *88*, 115205.
(54) Eda, G.; Yamaguchi, H.; Voiry, D.; Fujita, T.; Chen, M.; Chhowalla, M. *Nano Lett.* **2011**, *11*, 5111−5116.

DOI: 10.1021/acs.nanolett.6b04896
Nano Lett. 2017, 17, 1655−1659